

Attosecond Streak Camera

J. Itatani,¹ F. Quéré,¹ G. L. Yudin,¹ M. Yu. Ivanov,¹ F. Krausz,² and P. B. Corkum¹

¹*Steacie Institute for Molecular Sciences, National Research Council of Canada, Ottawa, Ontario, Canada K1A 0R6*

²*Institute für Photonik, Technische Universität Wien, Gusshausstrasse 27, A-1040 Wien, Austria*

(Received 29 August 2001; published 16 April 2002)

An electron generated by x-ray photoionization can be deflected by a strong laser field. Its energy and angular distribution depends on the phase of the laser field at the time of ionization. This phase dependence can be used to measure the duration and chirp of single sub100-attosecond x-ray pulses.

DOI: 10.1103/PhysRevLett.88.173903

PACS numbers: 42.65.Ky, 41.50.+h

Historically, advances in our ability to measure fast phenomena have led to corresponding scientific advances [1]. It is now possible to use the physics of high harmonic generation for producing single attosecond (10^{-18} sec, asec) pulses in the extreme ultraviolet to soft x-ray regions [2,3]. The next frontier will be to utilize such ultrashort pulses to probe the electronic dynamics of atoms and molecules which occurs on the attosecond time scale [4]. However, one impediment for experimentally demonstrating attosecond pulses has been the problem of finding a good method for their characterization [5–7].

We present a method to determine the duration and chirp of a single attosecond x-ray pulse, based on the ionization of atoms by the x-ray photons in the presence of a strong low-frequency laser field. This method relies on two basic ideas. (i) The subcycle oscillation of the laser electric field is used as a time reference to determine the duration of the x-ray pulse. This can be done only if the x-ray pulse is shorter than the period of the oscillating field. (ii) The photoelectron signal generated by the x-ray pulse is resolved in energy and angle simultaneously. Depending on the laser-field polarization, the information on the pulse duration is contained in the width of the energy spectrum at a given observation angle (linear polarization), or in the width of the angular distribution at a given energy (circular polarization). We show that the resolution limit depends on the photon energy, bandwidth, and chirp of the x-ray pulse. The resolution improves with increasing photon energy, and is on the order of 70 asec at 100 eV for transform-limited pulses.

A group including two of the authors has implemented a closely related configuration, where the photoelectrons are collected in the direction perpendicular to the laser polarization, and successfully characterized x-ray pulses shorter than one oscillation period of the laser field used for their generation [3,8].

The ionization of atoms by x rays in the presence of laser fields has been used for several years to measure the duration of x-ray pulses longer than the optical period of the laser field. In these measurements, Auger electrons [9] or x-ray photoelectrons [10–12] are dressed by the laser field to cross correlate the x-ray pulse and the envelope of the laser pulse. Two effects are used for this cross correlation.

(i) The appearance of sidebands in the photoelectron energy spectrum due to the emission and absorption of laser photons by the x-ray generated photoelectrons. (ii) The ponderomotive shift of these peaks, due to the ac Stark shift of the continuum induced by the laser field.

As shown later, as the pulse duration falls below one period of the laser radiation, the sidebands broaden and merge, and the ponderomotive shift is no longer observable. Therefore, these cross-correlation methods cannot be directly extended to subcycle x-ray pulses.

By analyzing the dynamics of the electrons, we will show how the laser field affects the photoelectron distribution in the case of subcycle x-ray pulses, and how this effect can be used to characterize these pulses. The large difference in frequencies between the x-ray pulse Ω_X and the laser pulse ω_L naturally divides the two-color ionization process in two steps: absorption of an x-ray photon followed by acceleration in the laser field [13]. The x ray produces an electron with a kinetic energy $W_0 = m_e v_0^2/2 = \hbar\Omega_X - I_p$, where I_p is the ionization potential and \mathbf{v}_0 is the initial velocity. If the $U_p \gg \hbar\omega_L$ and $\hbar\Omega_X \gg I_p$, classical mechanics can be used to determine the time-dependent velocity $\mathbf{v}(t)$ in the field [14,15]. For the laser electric field $\mathbf{E}_L(t) = E_0(t)/\sqrt{1 + \varepsilon^2} \{\cos(\omega_L t + \varphi)\mathbf{e}_x + \varepsilon \sin(\omega_L t + \varphi)\mathbf{e}_y\}$ with ellipticity ε , this velocity is expressed as

$$\mathbf{v}(t) = -\frac{e}{m_e} \mathbf{A}(t) + \left[\mathbf{v}_0 + \frac{e}{m_e} \mathbf{A}(t_i) \right], \quad (1)$$

where $\mathbf{A}(t)$ is the vector potential of the field, $\mathbf{E}_L = -\partial\mathbf{A}/\partial t$, and t_i is the time of ionization.

In Eq. (1) the first term describes the electron's quiver motion and goes to zero as the laser pulse ends. The second term is determined by the initial condition $\mathbf{v}(t_i) = \mathbf{v}_0$ at the time of ionization. This term is the final drift velocity $\mathbf{v}_f = \mathbf{v}_0 + (e/m_e)\mathbf{A}(t_i)$ measured after the laser pulse. The fact that \mathbf{v}_f is different from \mathbf{v}_0 is the classical equivalent to the absorption, emission, and scattering of laser photons by the photoelectron [13,16].

The dashed circle of radius v_0 in Fig. 1 shows the electron velocity distribution in the xy plane ($v_{0,z} = 0$) produced by the x rays alone. The solid circle in Fig. 1 represents the drift velocity distribution in the presence of

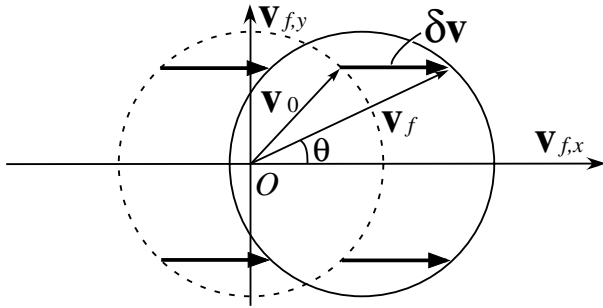


FIG. 1. Effect of a strong laser field on the photoelectrons ionized by the x-ray pulse at a given phase ϕ_i . Dashed circle—drift velocity distribution (v_{0x}, v_{0y}) of the photoelectrons without the laser field; solid circle—distribution with the laser field. Note that neither the uncertainty in \mathbf{v}_0 due to the bandwidth of the x-ray pulse nor the angular dependence of the emission probability are represented for simplicity.

the laser field. It is a translation of the dashed circle by $\delta\mathbf{v} = (e/m_e)\mathbf{A}(t_i)$. For linearly polarized light ($\varepsilon = 0$), the translation is parallel to the electric field, and the electron distribution sweeps back and forth along the field direction as t_i varies. For circularly polarized light ($\varepsilon = \pm 1$), the electron distribution is displaced perpendicular to the laser electric field at the moment of birth, and it rotates around the dashed circle as the time of ionization is varied.

For all polarizations, electrons that are freed at slightly different times t_i will have different final velocities because of the dependence of \mathbf{v}_f on the optical phase $\phi_i = \omega_L t_i + \varphi$. It is this phase dependence that offers an opportunity for the measurement of subcycle duration. To evaluate the temporal resolution, it is convenient to reformulate Eq. (1) in terms of the drift kinetic energy $K = m_e v_f^2/2$ for electrons moving in the xy plane:

$$\begin{aligned} K_L &= W_0 + 2U_p \cos 2\theta \sin^2 \phi_i \pm \alpha_L \sqrt{8W_0 U_p} \cos \theta \sin \phi_i, \\ K_C &= W_0 - U_p \cos 2(\phi_i - \theta) \pm \alpha_C \sqrt{4W_0 U_p} \sin(\phi_i - \theta), \\ \alpha_L &= \{1 - (2U_p/W_0) \sin^2 \theta \sin^2 \phi_i\}^{1/2}, \quad \alpha_C = \{1 - (U_p/2W_0) - (U_p/2W_0) \cos[2(\phi_i - \theta)]\}^{1/2}. \end{aligned} \quad (2)$$

Here K_L, K_C are the kinetic energies for linear and circular polarization of the laser field, respectively; $U_p = e^2 E_0^2(t_i)/4m_e \omega_L^2$ is the ponderomotive potential of the laser field at the time of ionization; θ is the angle of observation measured from the x axis as shown in Fig. 1; α_L and α_C are correction terms to the expression given in [8], and deviate from 1 when U_p becomes comparable to or higher than W_0 . If the field is increased to $U_p > W_0/2$ (linear polarization) or $U_p > W_0$ (circular polarization), some of the photoelectrons are deflected into the reverse direction from $\mathbf{v}(t_i) = \mathbf{v}_0$. The branches of negative signs account for these backscattered electrons, and are required only for this high intensity regime. In this case, another peak appears on the lower energy side of photoelectron spectra, which makes their interpretation more complex. Hereafter, we will restrict the discussion to $U_p < W_0/2$ (linear polarization) and $U_p < W_0$ (circular polarization).

There are many possibilities for measurement because the photoelectron spectra depend on the observation angle and the laser polarization. We will concentrate on three configurations. For a linearly polarized field, if we observe only electrons with \mathbf{v}_f parallel to the laser polarization, Eq. (2) shows that the drift energy will sweep above and below W_0 as the phase of birth varies from 0 to 2π . If we observe only electrons with \mathbf{v}_f perpendicular to the laser polarization, Eq. (2) shows that it will sweep only below W_0 twice per laser period. Measurements that are angle integrated will have a degraded resolution. In circularly polarized light, if we observe only electrons of a given energy, then their direction will sweep. For any polarization, measurements that are energy integrated [5] will have a degraded resolution.

With a linearly polarized field, the width ΔE of the angle-resolved photoelectron spectrum is determined by the following factors: (i) the variation of the moment of birth of photoelectrons due to the x-ray pulse duration, and (ii) the bandwidth and the chirp of the x-ray pulse. Thus, the duration and chirp can be determined by comparing the spectra with and without the laser field.

For a transform-limited x-ray pulse, the width of a photoelectron spectrum is given as $\Delta E[\tau_X, \Delta(\hbar\Omega_X)] = \{(|\partial K/\partial \phi_i| \omega_L \tau_X)^2 + [|\partial K/\partial W_0| \Delta(\hbar\Omega_X)]^2\}^{1/2}$ provided that the streaking speed $\partial K/\partial \phi_i$ is constant within the x-ray pulse. Within one optical period, the best temporal resolution is achieved at the phase that maximizes the resolving parameter $\beta_L \equiv (|\partial K/\partial \phi_i| \omega_L \tau_X) / \{|\partial K/\partial W_0| \Delta(\hbar\Omega_X)\}$. It occurs at $\phi_i = m\pi$ for $\theta = 0$ or $\phi_i = (m/2 + 1/4)\pi$ for $\theta = \pi/2$, respectively. β_L scales as $v_0 E_0(t_i) \tau_X^2$ for $\theta = 0$ and $E_0^2(t_i) \tau_X^2$ for $\theta = \pi/2$. Physically, as the x-ray pulse duration decreases, its bandwidth increases as $\propto 1/\tau_X$ and the contribution of sweeping to the photoelectron bandwidth ΔE decreases as $\propto \tau_X$.

We set the condition for the resolution limit as $\beta_L = 1$, i.e., the x-ray bandwidth is equal to the broadening by the laser streak. This is the criterion used in traditional streak cameras. For transform-limited x-ray pulses at 100 eV, the resolution limit is 70 asec for $\theta = 0$ and 100 asec for $\theta = \pi/2$. Here we assumed helium as an ionizing atom ($I_p = 24.6$ eV), laser wavelength $\lambda_L = 0.8 \mu\text{m}$, and the intensity of the laser field set by $U_p = W_0/2$ ($I = 6.3 \times 10^{14}$ W/cm²).

One drawback of using a linearly polarized laser field is that the streaking speed $\partial K/\partial \phi_i$ varies within the laser period, as seen in Eq. (2). If the x-ray pulse duration

becomes close to the streaking period, the streaking speed will change within the x-ray pulse, which will make the data interpretation more complicated. This difficulty can be removed by using a circularly polarized laser field.

With circularly polarized light, a photoelectron at a given kinetic energy streaks in angle as shown in Eq. (2). This angular spread $\Delta\theta$ of photoelectron distribution in the xy plane can be used to measure the duration of x-ray pulses. The main advantage of this configuration is that the streaking speed is constant over the whole optical cycle, and is automatically calibrated by the frequency of the laser field. This method generalizes the concept of the attosecond streak camera [5], which is based on the measurement of the angular distribution of photoelectrons without resolving the kinetic energy. Energy-integrated measurements require $U_p \gg W_0$, a condition difficult to achieve experimentally. The temporal resolution of this configuration is again limited by the bandwidth of the x-ray pulse and is similar to that for linear polarization (70 asec for 100 eV photons).

The electron spectrum can also be calculated quantum mechanically [atomic units are used for compactness in Eqs. (3) and (4)]. Following [17], the amplitude of populating a state $|\mathbf{v}\rangle$ with kinetic momentum \mathbf{v} at a moment T after the end of both the laser and the x-ray pulses is

$$a_{\mathbf{v}}(T) = -i \int_{-\infty}^T dt \mathbf{d}_{\mathbf{p}(t)} \mathbf{E}_X(t) e^{-i \int_t^T dt' (1/2[\mathbf{p}(t')]^2 + I_p)}, \quad (3)$$

where $\mathbf{p}(t) = \mathbf{v} + \mathbf{A}(t)$ is the instantaneous kinetic momentum, and $\mathbf{d}_{\mathbf{p}(t)}$ is the dipole transition matrix element from the ground state to the continuum with kinetic momentum $\mathbf{p}(t)$. The x-ray field $\mathbf{E}_X(t)$ includes the fast oscillations of the carrier, chirp, and the pulse envelope.

We assume that the x-ray pulse is a linearly chirped Gaussian, with dimensionless chirp ξ defined in the spectral domain as $\tilde{E}_X(\Omega) \sim \exp[-(\Omega - \Omega_X)^2 \tau^2 (1 - i\xi)/2]$. In time domain, positive chirp $\xi > 0$ corresponds to the instantaneous frequency increasing with time: $E_X(t) \sim \exp[-(t - t_0)^2 (1 + i\xi)/2\tau^2 (1 + \xi^2) - i\Omega_X t]$, where t_0 is the peak of the x-ray pulse and its duration is $\tau_X \sim \tau\sqrt{1 + \xi^2}$. For a sufficiently short x-ray pulse, Eq. (3) can be approximated using the saddle point method, so we have

$$|a_{\mathbf{v}}|^2 \propto \frac{|\mathbf{d}_{\mathbf{p}(t_0)} \mathbf{E}_X(t_0)|^2}{\mu} \exp\left[-\left(\frac{\mathbf{p}^2(t_0)}{2} - W_0\right)^2 \frac{\tau^2}{\mu^2}\right], \quad (4)$$

$$\mu = \sqrt{(1 + \eta\xi)^2 + \eta^2}, \quad \eta = \mathbf{E}_L(t_0) \mathbf{p}(t_0) \tau^2.$$

Equations (3) and (4) apply for all directions of observation and laser polarizations. In the field-free case $\mu = 1$ and Eq. (4) corresponds to the spectrum of the x-ray pulse shifted by $-I_p$. Equation (4) shows that, in the presence of the laser pulse, the width of the electron spectrum depends on $\mathbf{E}_L(t_0)$ at the peak of the x-ray pulse. To measure the x-ray pulse duration, one must produce an observable change in μ .

Figure 2a shows photoelectron spectra in the direction parallel to the laser polarization produced by 70 asec (full width at half maximum, FWHM) transform-limited x-ray pulses for the same condition that we used to derive the resolution limit above. The center of the x-ray pulse is set at the maximum of the laser field ($\omega_L t_0 + \varphi = 0$). The solid curve corresponds to the field-free spectrum. In the presence of the laser field, classical [open circles, from Eq. (2)] and quantum-mechanical [dotted curve, from Eq. (3)] calculations agree well. The laser field broadens the spectrum by $\sqrt{2}$ as predicted in the semiclassical analysis above.

In the case of a chirped x-ray pulse, substantial modification of the spectrum can be achieved when $\eta\xi \sim 1$, which for large chirps allows one to deal with larger bandwidth $\Delta\Omega_X \sim 1/\tau$. Physically, if the photoelectrons are positively streaked ($\partial K/\partial\phi_i > 0$), the width of the photoelectron spectrum will be larger than the transform-limited case for positive chirp of the x-ray pulse, and narrower for negative chirp. Equation (4) allows us to determine both the sign and the magnitude of the chirp.

Figure 2b shows the photoelectron spectra produced by chirped x-ray pulses (70 asec FWHM, $\xi = \pm\sqrt{3}$). The spectra are calculated using Eq. (3) [Eq. (4) gives almost identical results]. Other conditions are the same as in

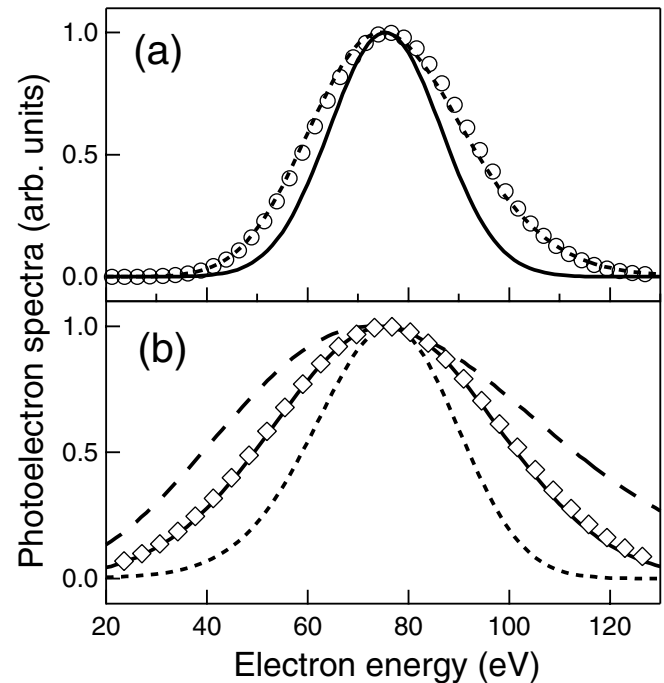


FIG. 2. (a) The photoelectron spectra produced by a transform-limited x-ray pulse (70 asec FWHM). Solid curve—field-free case; dotted curve—with a laser field ($I = 6.3 \times 10^{14}$ W/cm²). The classical result is shown by open circles. (b) The photoelectron spectra produced by chirped x-ray pulses (70 asec FWHM, $\xi = \pm\sqrt{3}$). Solid curve—field-free case; dashed curve is for the positive chirp; dotted curve is for the negative chirp. Open diamonds are for the transform-limited case (35 asec FWHM, $\xi = 0$). The field intensity is the same as in (a).

Fig. 2a. The solid line shows the field-free photoelectron spectrum. Depending on the sign of the chirp, we can clearly see the broadening or narrowing of the spectrum. For a transform-limited pulse (35 asec FWHM, $\xi = 0$), the broadening can hardly be seen (open diamonds in Fig. 2b).

In the above analysis, we have made a number of implicit assumptions that might influence experiments. Shot-to-shot fluctuation of the streaking phase ϕ_i will increase the width of the photoelectron spectra and degrade the temporal resolution. In high harmonic generation, the most likely source of attosecond pulses, the x-ray pulses are naturally phase locked to the driving laser pulses. Therefore, the combination of these x-ray and laser pulses is ideal for the attosecond streak camera. Fluctuation of the field intensity ($\propto U_p$) will also degrade the resolution. However, with Ti:sapphire lasers we can expect a good stability of $\sim 5\%$.

The maximum temporal resolution requires the highest feasible intensity of the laser field. Above-threshold ionization (ATI) by the laser field alone can produce a significant number of background electrons which limit the intensity that can be used. There are three ways to minimize the influence of ATI electrons. (i) A few-cycle laser pulse reduces the total ionization probability at a given intensity [8]. (ii) ATI tends to produce low energy electrons directed along the laser polarization. The energy and angle of observation can be chosen to reduce their influence [8]. (iii) For the linearly polarized case, the small background of rescattered electrons can be suppressed by introducing a slight ellipticity to the field.

Angular dependence of the photoionization cross section may seem to present a problem for correctly interpreting the observed photoelectron spectrum. However, it is technically feasible to cancel this anisotropy by integrating the photoelectron signal while rotating the polarization of the x-ray pulse with respect to the laser polarization. In the case of high harmonics, this can be done by rotating the polarization direction of the laser pulses used for x-ray generation.

Before concluding, we revisit the multicycle measurements from a subcycle perspective. As we have seen, the strong laser field distorts the photoelectron spectrum on the subcycle time scale. This effect corresponds to a frequency modulation of the photoelectron wave function within the laser optical cycle. If the x-ray pulse is longer than the laser period τ_L , this modulation is repeated identically every optical cycle. This leads to a temporal periodicity of the wave function, which is responsible for the appearance of sidebands spaced by $\hbar\omega_L$ in the energy spectrum.

The positions of the sidebands are determined by the phase shift of the wave function that occurs from one optical cycle to the following one. This is analogous to the frequency comb spectrum of a pulse train from a mode-locked

laser. The position of the comb is determined by the shift of the carrier-envelope optical phase from pulse to pulse [18,19]. For the electrons, a similar phase shift occurs because an electron born at time t makes one oscillation more in the laser field than one born at $t + \tau_L$. The quantum phase acquired during this extra oscillation is $2\pi U_p/\hbar\omega_L$, and accounts for the ponderomotive shift of the sidebands by $-U_p$.

In conclusion, the attosecond streak camera will allow resolution ≤ 100 asec. To realize this resolution experimentally, any phase variation of the laser field with respect to the x-ray pulse must be less than $2\pi(\tau_X/\tau_L)$ over the interaction volume and between laser shots. This criterion appears achievable for attosecond x-ray pulses produced by high harmonic generation.

This work is supported in part by Photonics Research Ontario.

Note added.—Recently isolated attosecond pulses [3] as well as a train of pulses [20] were successfully characterized using x-ray photoionization of atoms in a laser field. The former [3] is closely related to our proposed method, but utilizes the broadening of photoelectron spectra due to a large angle of collection. The latter [20] is not directly related to our method, but, by using Eq. (3), this experiment can be understood as the interference of photoelectron wave packets with laser-induced phase shifts (see also [21]).

-
- [1] A. H. Zewail, *J. Phys. Chem. A* **104**, 5660 (2000).
 - [2] T. Brabec and F. Krausz, *Rev. Mod. Phys.* **72**, 545 (2000), and references therein.
 - [3] M. Hentschel *et al.*, *Nature (London)* **414**, 509 (2001).
 - [4] F. Krausz, *Phys. World* **14**, 41 (2001).
 - [5] E. Constant *et al.*, *Phys. Rev. A* **56**, 3870 (1997).
 - [6] Y. Kobayashi *et al.*, *Opt. Lett.* **23**, 64 (1998).
 - [7] A. Scrinzi, M. Geissler, and T. Brabec, *Phys. Rev. Lett.* **86**, 412 (2001).
 - [8] M. Drescher *et al.*, *Science* **291**, 1923 (2001).
 - [9] J. M. Schins *et al.*, *Phys. Rev. Lett.* **73**, 2180 (1994).
 - [10] T. E. Glover *et al.*, *Phys. Rev. Lett.* **76**, 2468 (1996).
 - [11] A. Bouhal *et al.*, *J. Opt. Soc. Am. B* **14**, 950 (1997).
 - [12] E. S. Toma *et al.*, *Phys. Rev. A* **62**, 061801(R) (2000).
 - [13] A. M. Dykhne and G. L. Yudin, *Usp. Fiz. Nauk* **121**, 157 (1977) [*Sov. Phys. Usp.* **20**, 80 (1977)]; *Usp. Fiz. Nauk* **125**, 377 (1978) [*Sov. Phys. Usp.* **21**, 549 (1978)].
 - [14] T. F. Gallagher, *Phys. Rev. Lett.* **61**, 2304 (1988).
 - [15] P. B. Corkum, N. H. Burnett, and F. Brunel, *Phys. Rev. Lett.* **62**, 1259 (1989).
 - [16] E. Yablonovitch, *Phys. Rev. Lett.* **60**, 795 (1988).
 - [17] M. Lewenstein *et al.*, *Phys. Rev. A* **49**, 2117 (1994).
 - [18] D. J. Jones *et al.*, *Science* **288**, 635 (2000).
 - [19] A. Apolonski *et al.*, *Phys. Rev. Lett.* **85**, 740 (2000).
 - [20] P. M. Paul *et al.*, *Science* **292**, 1689 (2001).
 - [21] F. Quéré *et al.* (to be published).